Remote Sensing of Environment 121 (2012) 516–526

Contents lists available at SciVerse ScienceDirect

Remote Sensing of Environment

journal homepage: www.elsevier.com/locate/rse

Image texture as a remotely sensed measure of vegetation structure

Eric M. Wood [a,*], Anna M. Pidgeon [a], Volker C. Radeloff [a], Nicholas S. Keuler [a,b]

[a] Department of Forest and Wildlife Ecology, University of Wisconsin–Madison, 1630 Linden Drive, Madison, WI 53706, USA
[b] Department of Statistics, University of Wisconsin–Madison, 1300 University Ave, Madison, WI 53706, USA

ARTICLE INFO

Article history:
Received 25 March 2011
Received in revised form 4 January 2012
Accepted 8 January 2012
Available online 5 March 2012

Keywords:
Band 4
Foliage-height diversity
Horizontal vegetation structure
Image texture
Infrared air photo
Landsat
NDVI
Wildlife habitat

ABSTRACT

Ecologists commonly collect data on vegetation structure, which is an important attribute for characterizing habitat. However, measuring vegetation structure across large areas is logistically difficult. Our goal was to evaluate the degree to which sample-point pixel values and image texture of remotely sensed data are associated with vegetation structure in a North American grassland–savanna–woodland mosaic. In the summers of 2008–2009 we collected vegetation structure measurements at 193 sample points from which we calculated foliage-height diversity and horizontal vegetation structure at Fort McCoy Military Installation, Wisconsin, USA. We also calculated sample-point pixel values and first- and second-order image texture measures, from two remotely sensed data sources: an infrared air photo (1-m resolution) and a Landsat TM satellite image (30-m resolution). We regressed foliage-height diversity against, and correlated horizontal vegetation structure with, sample-point pixel values and texture measures within and among habitats. Within grasslands, savanna, and woodland habitats, sample-point pixel values and image texture measures explained 26–60% of foliage-height diversity. Similarly, within habitats, sample-point pixel values and image texture measures were correlated with 40–70% of the variation of horizontal vegetation structure. Among habitats, the mean of the texture measure 'second-order contrast' from the air photo explained 79% of the variation in foliage-height diversity while 'first-order variance' from the air photo was correlated with 73% of horizontal vegetation structure. Our results suggest that sample-point pixel values and image texture measures calculated from remotely sensed data capture components of foliage-height diversity and horizontal vegetation structure within and among grassland, savanna, and woodland habitats. Vegetation structure, which is a key component of animal habitat, can thus be mapped using remotely sensed data.

© 2012 Elsevier Inc. All rights reserved.

1. Introduction

Vegetation structure is an important attribute of wildlife habitat quality (Cody, 1981, 1985; MacArthur & MacArthur, 1961; Morrison et al., 2006; Nudds, 1977) and vegetation structure characteristics partition animal species both within and among habitats (Hutto, 1985; Rotenberry & Wiens, 1980; Wiens & Rotenberry, 1981). Throughout their lives, animals make habitat selection decisions at multiple scales (Morrison et al., 2006). For example, at broad scales, landbirds select habitat types with strongly different structural characteristics, such as a grassland or woodland (Cody, 1985). At fine scales, differences in vertical and horizontal vegetation structure are strongly associated with nest placement (Martin, 1993), and foraging site selection during migration (Hutto, 1985) and the breeding season (Robinson & Holmes, 1984). Thus, in the half century since MacArthur and MacArthur (1961) put forth their hypothesis that vegetation structure influences avian diversity, this relationship has become a central tenet of wildlife habitat selection theory (Morrison et al., 2006; Tews et al., 2004).

The measure *foliage-height diversity*, (MacArthur & MacArthur, 1961), or derivations of this measure, are commonly used to characterize vegetation structure. Foliage-height diversity quantifies vertical heterogeneity in vegetation structure at a given point. Furthermore, multiple measures of foliage-height diversity can be used jointly to derive an index of horizontal vegetation structure depicting the variation in canopy heights within a habitat patch (Wiens & Rotenberry, 1981). Similar indices of heterogeneity in horizontal vegetation structure such as cover-board measurements are linked with habitat density and patchiness (Nudds, 1977), which are useful descriptors for wildlife occurrence (McShea, 2000). Foliage-height diversity is a flexible measure that can describe avian habitat in ecosystems from sparse grasslands (Patterson & Best, 1996; Rotenberry & Wiens, 1980; Wiens & Rotenberry, 1981), to patchy deserts (Pidgeon et al., 2001), and dense forests (Estades, 1997; Karr & Roth, 1971). In addition, foliage-height diversity can characterize habitat for tropical mammal communities (August, 1983), ant biodiversity in grazed and ungrazed habitats (Bestelmeyer & Wiens, 2001), spider communities (Greenstone, 1984), and insect diversity (Murdoch et al., 1972; Southwood et al., 1979). However, while foliage-height diversity is a

* Corresponding author. Tel.: +1 608 265 9219; fax: +1 608 262 9922.
E-mail address: emwood@wisc.edu (E.M. Wood).

0034-4257/$ – see front matter © 2012 Elsevier Inc. All rights reserved.
doi:10.1016/j.rse.2012.01.003

key measure for describing wildlife habitat, it is labor intensive to collect and consequently is mainly limited to small scale studies. Therefore, ecologists need efficient methods for characterizing foliage-height diversity, and its derived measures, at a sufficiently fine grain yet broad extent to be useful for management and conservation applications.

Remotely sensed data are powerful for characterizing habitat at broad extents, for example to describe landscape configuration (Kerr & Ostrovsky, 2003; Turner et al., 2001) and for assessing biodiversity (Gillespie et al., 2008; Laurent et al., 2005; Roughgarden et al., 1991; Turner et al., 2003). Broad scale land cover classifications are useful predictors of wildlife occurrence (Anderson, 1976; Thuiller et al., 2004; Venier et al., 2004). Indices derived from remotely sensed data sources, such as the normalized difference vegetation index (NDVI), which is a proxy for vegetative cover and productivity, are associated with patterns of wildlife species richness (Bailey et al., 2004; Seto et al., 2004; St-Louis et al., 2009), and habitat suitability at broad spatial extents (Naugle et al., 1999). Additionally, Light Detection and Ranging (LiDAR) can characterize vegetation heights at smaller spatial resolutions, which are positively associated with animal distributions (Vierling et al., 2008), occurrence (Seavy et al., 2009), diversity (Clawges et al., 2008; Goetz et al., 2007; Lesak et al., 2011), and habitat quality (Goetz et al., 2010; Hinsley et al., 2006). However, among the remote sensing data that are used to characterize wildlife habitat, LiDAR and Synthetic Aperture Radar (SAR) are the only products from which foliage-height diversity can be mapped (Bergen et al., 2009; Clawges et al., 2008). Unfortunately though, while SAR data are widely available, LiDAR data are not. Furthermore, there are limited image archives for LiDAR, in contrast to satellite imagery (e.g., Landsat TM), thus it is not possible to analyze change in vegetation structure over time.

However, while optical satellite data or air photos cannot measure vegetation height directly, remotely sensed image texture may be a good proxy of vegetation structure. Image texture has been used to characterize distributions of landbirds in heterogeneous habitat types including eastern North American deciduous and coniferous forests (Culbert et al., 2009; Hepinstall & Sader, 1997; Tuttle et al., 2006), desert shrublands and grasslands (St-Louis et al., 2006, 2009), and agricultural grassland ecosystems (Bellis et al., 2008), and habitat selection patterns of the endangered mountain bongo (*Tragelaphus eurycerus isaaci*) in east African montane forests (Estes et al., 2008, 2010). Image texture measures the heterogeneity in the tonal values of pixels within a defined area of an image. Image texture data is fine grained, depending on the image resolution, yet broad in extent, a combination of attributes that are desirable for landscape-scale characterization of wildlife habitat.

In addition to its use in characterizing animal distribution patterns, image texture has also been used for characterizing vegetation patterns (Ge et al., 2006) and as input for vegetation classifications, for example in the Canadian Rocky Mountains (Zhang & Franklin, 2002), Canadian coastal forests (Coburn & Roberts, 2004), African grasslands and savannas (Hudak & Wessman, 1998, 2001), and African montane habitats (Estes et al., 2008, 2010). However, to our knowledge, no study has directly evaluated the use of image texture for quantifying vegetation structure as represented by foliage-height diversity. This relationship is important to understand because it is presumably the ability of image texture to measure vegetation structure that underlies its strong correlation with wildlife diversity measures.

Our goal was to evaluate the strength of the relationship of remotely sensed pixel values and image texture measures, calculated from air photos and satellite images, with foliage-height diversity and horizontal vegetation structure that are widely used to characterize wildlife habitat. We conducted this analysis in a North American grassland–savanna–woodland mosaic where the wide range of vegetation structural characteristics provided an appropriate setting for testing these relationships. Our specific objectives were 1) to determine which sample-point pixel value summaries and image texture measures derived from air photos and Landsat TM data were best at characterizing foliage-height diversity and horizontal vegetation structure both within and among habitats and 2) to offer recommendations for using remotely sensed measures of texture in wildlife habitat models.

2. Materials and methods

2.1. Study site

Our study area was the 24, 281 ha Fort McCoy Military Installation, in the Driftless Area of southwestern Wisconsin, USA (Fig. 1). The dominant habitat types at Fort McCoy include grasslands (defined here as less than 5% tree canopy cover), composed of grasses and forbs with intermittent patches of bare ground and low shrub cover; oak savannas (5–50% tree canopy cover with variable shrub cover), and woodlands (>50% tree canopy cover with variable shrub cover, Curtis 1959, Fig. 2). Dominant tree species include black oak (*Quercus velutina*), northern pin oak (*Quercus ellipsoidalis*), bur oak (*Quercus macrocarpa*), jack pine (*Pinus banksiana*), black cherry (*Prunus serotina*), red oak (*Quercus rubra*), and white oak (*Quercus alba*). Dominant shrubs include blueberry (*Vaccinium angustifolium*) and American hazelnut (*Corylus americana*), while dominant grasses include big bluestem (*Andropogon gerardii*) and little bluestem (*Schizachyrium scoparium*).

Fort McCoy is an operational military installation and approximately 50% of its area is off limits to non-military personnel. Of the remaining area, roughly 16% is grassland, 24% is oak savanna, and 40% is oak woodland. Small patches of cattail marshes, riparian tracts, and bogs make up the remaining 20%. Within these areas, a stratified random sampling design was used to select points for ground based foliage-height diversity quantification and image texture calculation. Three habitat types, grassland, oak savanna (hereafter savanna), and oak woodland (hereafter woodland) were classified using an infrared air photo and a digital raster graphic map depicting land cover types.

Polygons encompassing patches of the three focal habitat types were manually digitized. Within the digitized polygons, 400 random sample points were generated using Hawth's Tools extension (Beyer, 2004) in ArcGIS 9.1 (ESRI, Redlands, California, USA, 2006). Reflectance of roads or other non-vegetative areas (i.e., buildings) can influence texture calculations, so all sample points that were within 150 m of a paved road or human structures were removed from consideration. Sample points that were located within 150 m of marginal roads (i.e., non-paved, single vehicle tracts) were included in this analysis because marginal roads were similar in their effect on image texture to naturally occurring bare areas. From this set, sample points that were surrounded by at least 100 m of one habitat type, and that were separated from other sample points by at least 300 m, were retained. This resulted in a total of 193 sample points, with 49 sample points in grassland, 84 in savanna, and 60 in woodland (Fig. 1).

2.2. Foliage-height diversity field measurements

Foliage-height diversity was measured, following the methods of Martin et al. (1997), at each sample point once from mid-June to late July in 2008 or 2009, which corresponded to the peak growing season for vegetation at our study area. Mean temperatures from March 1 to August 15, which corresponded to the time frame ranging from the early spring thaw to the duration of our foliage-height diversity sampling, were not significantly different between 2008 (10.94 °C) and 2009 (11.23° C, $t_{167} = -0.60$, $p = 0.55$). Similarly, mean precipitation of 2008 (log transformed, 0.35 mm) and 2009

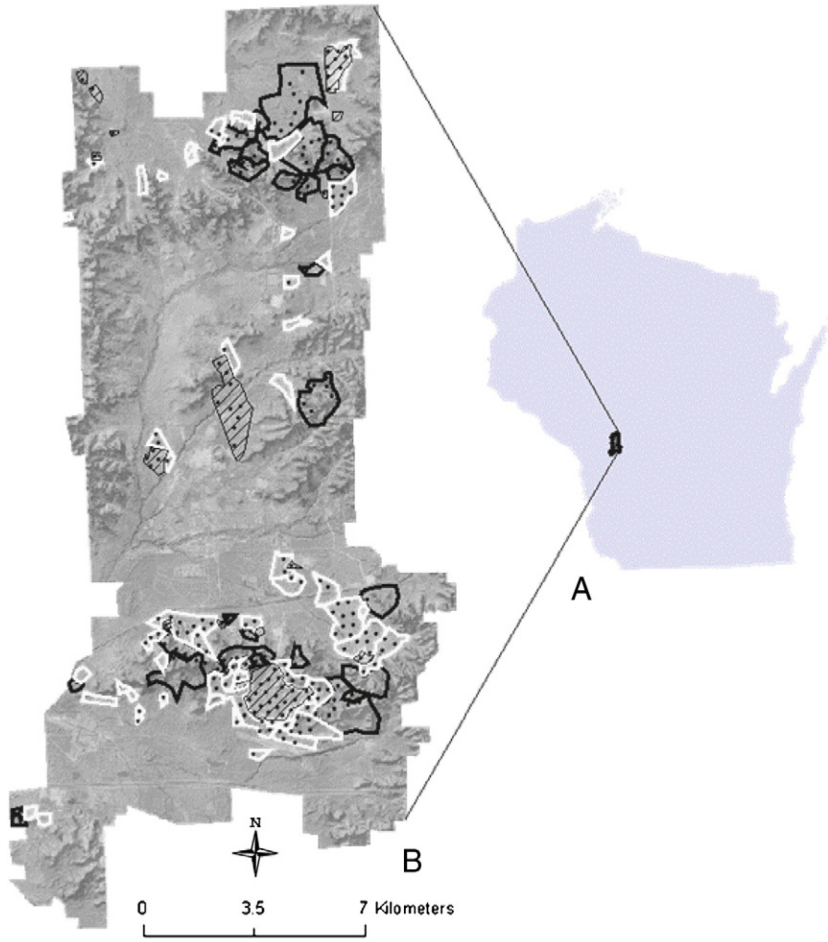

Fig. 1. A) Fort McCoy Military Installation, Wisconsin, USA. B) Distribution of 193 sample points where foliage-height diversity data was collected and texture values were calculated. The sample points were distributed across an open to dense tree canopy cover gradient in three habitat types, 1) grasslands denoted by barred polygons, 2) savanna denoted by white outlined polygons, and 3) woodlands denoted by black outlined polygons. A hillshade model was calculated from a digital elevation model and set underneath a 60% transparent air photo to better show topographical features of Fort McCoy.

(log transformed, 0.51 mm) was not significantly different ($t_6 = -0.04$, $p = 0.98$).

At each sample point, measurements were collected at four 5-m radius sub-plots, located at the center of the sample point and with one each at azimuth angles of 0°, 120°, and 240°, at a random distance between 20 and 80 m. These random distances were chosen so all foliage-height diversity measurements were entirely within the 100-m radius sample plot. We used random distances to select sub-plots because although vegetation structure was homogenous in the grassland it was heterogeneous in the savanna and woodland and this structural variation was best characterized using a random distance sampling protocol (Fig. 2). From the center point of each sub-plot, one observer walked 5 m in each of the cardinal directions and a 12-m tall telescoping pole marked at 30-cm intervals was placed vertically on the ground. A second observer recorded the number of hits (i.e., instances where vegetation touched the pole) in each 30 cm section. If the canopy was taller than 12 m, then the second observer stood 5 m from the base of the telescoping pole in an area where the view of the telescoping pole was not obscured by vegetation and used binoculars to estimate vegetation hits at approximate 30-cm intervals. Tree heights in the savanna ranged from 4 to 17 m and from 5 to 25 m for the woodland habitat. In the savanna, observers estimated tree heights above the 12 m tall telescoping pole at approximately 40% of the sub-plots. In the woodland, observers estimated tree heights at approximately 75% of the sub-plots. This yielded four measurements at each of the four sub-plots totaling 16 foliage-height profiles at each sample point.

From these 16 foliage-height tallies two indices of vegetation structure were calculated. First, foliage-height diversity was computed using the Shannon diversity index (MacArthur & MacArthur, 1961) using the formula:

$$H' = -\sum_{i=1}^{k} (p_i \ln p_i)$$

where k was the total number of 'hits' of vegetation along the foliage-height diversity pole and p_i was the proportion of 'hits' found in category i (Zar, 1999). Second, horizontal vegetation structure was derived by taking the standard deviation of canopy height at the 16 foliage-height diversity measurements per sample point (Wiens & Rotenberry, 1981).

2.3. Remote sensing data sources

A leaf-on, 1-m resolution, infrared air photo taken in late August 2006, the near-infrared Band 4 from a Landsat TM (hereafter Landsat) scene acquired July 13, 2009 (path 25, row 29), and a NDVI calculated from the Landsat scene were the basis of our image texture analyses. The images were captured during the middle of the growing season for trees and shrubs in our study area. We used the infrared air photo (hereafter air photo), and Band 4 from the Landsat scene because green vegetation strongly reflects near-infrared light (Gausman, 1977), which led us to the hypothesis that these image

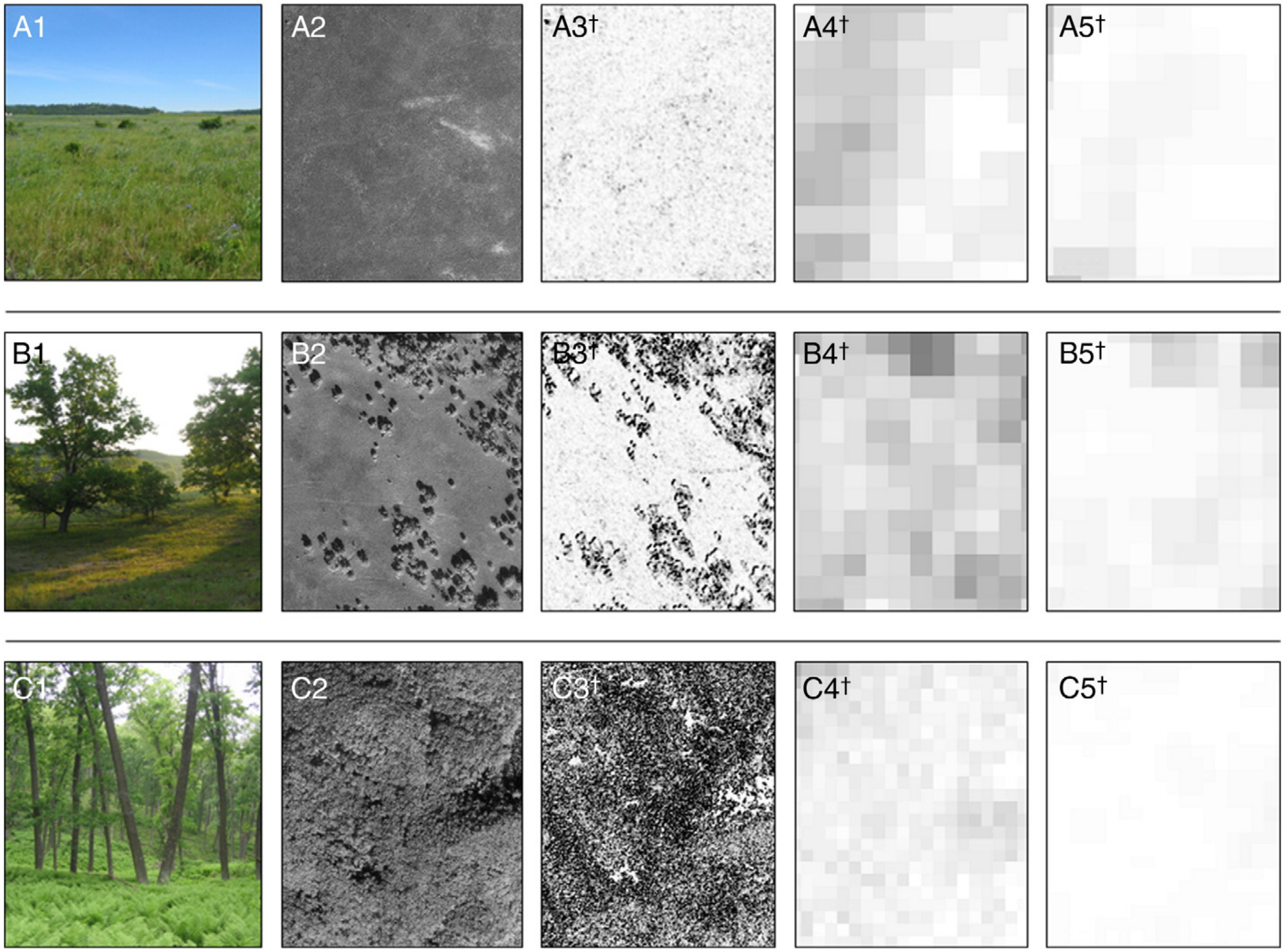

Fig. 2. A) Grassland, B) savanna, and C) woodland. Each habitat type depicted with a 1) ground photo, 2) a 1 m resolution infrared air photo, 3) infrared air photo-derived 2nd order contrast calculated in a 3 × 3 moving window, 4) NDVI calculated from a Landsat scene, and 5) NDVI-derived 2nd order contrast calculated in a 3x3 moving window. In images with cross (†) the color ramp was stretched and inverted for clearer display.

sources would be related to foliage-height diversity and horizontal vegetation structure. Furthermore, because wildlife responds to vegetation productivity and greenness (Lee et al., 2004; Seto et al., 2004; Szép et al., 2006), we used the NDVI (Tucker, 1979). There were no significant disturbances (e.g., thinning or fire) at our sample points between the time the air photo or the satellite imagery were captured and the foliage-height diversity measurements were collected. Furthermore, the dominant trees of our study area (e.g., black oak) likely grew very little over the duration of the study. Thus, the vegetation was similar between the time the imagery was captured and the foliage height diversity measurements were collected.

2.4. Image texture analysis

Image texture was calculated in 100-m radius sample-point summaries of pixel values and in a moving window analysis of first-order (occurrence) and second-order (co-occurrence) statistics (Haralick, 1979; Haralick et al., 1973). For sample-point summaries, the mean and the standard deviation of the pixel values within 100 m of a sample point were summarized (hereafter sample-point mean or standard deviation).

To compute first-order statistics for a given scale of interest (e.g., a 3 × 3 pixel window), the pixel values within a moving window were used to calculate a statistic (e.g., variance), which was assigned to the central pixel. Second-order statistics consider the spatial relationships among neighboring pixels (Hall-Beyer, 2007; Haralick, 1979; Haralick et al., 1973). To calculate second order statistics, the pixel values for a given scale of interest were first translated into a gray-level co-occurrence matrix (GLCM). The texture statistics were calculated based on the GLCM (Hall-Beyer, 2007). Image texture was calculated for every pixel using ENVI software (Research Systems Inc., Boulder, Colorado).

To match the scale at which our ground-collected vegetation structure data were collected and image texture was calculated, we applied a 3 × 3 window size for all image texture analyses. This window size has the advantage of capturing heterogeneity of pixel values over small extents. Vegetation structure varies abruptly in our study system (e.g., individual or small groups of shrubs or trees located in savanna habitat), suggesting that a small window size matches the scale of the vegetation structure patterns best.

Texture measures were selected based on their established ability to characterize vegetation structure (Dobrowski et al., 2008; Ge et al., 2006; Kuplich et al., 2005; Lu & Batistella, 2005; Tuominen & Pekkarinen, 2005). We calculated three first-order texture measures (entropy, mean, and variance), and eight second-order texture measures (angular second moment, contrast, correlation, dissimilarity, entropy, homogeneity, mean, and variance, Table 1) on the air photo, Band 4, and the NDVI. The tool 'zonal statistics' in ArcGIS 9.1 was used to summarize the mean and standard deviation of each texture measure within 100 m of each sample point.

Table 1
Eight second-order measures of image texture calculated from a gray-level co-occurrence matrix (GLCM) with description of what they measure, and the statistic formula.

Second-order statistic	Statistic description of behavior	Statistic formula[a]
Angular-second moment	High when the GLCM is locally homogenous. Similar to Homogeneity.	$\sum_i \sum_j \{p(i,j)\}^2$
Contrast	A measure of the amount of local variation in pixel values among neighboring pixels. It is the opposite of homogeneity.	$\sum_{n=0}^{N-1} n^2 \left\{ \sum_{i=1}^{N} \sum_{j=1}^{N} p(i,j) \right\}$
Correlation	Linear dependency of pixel values on those of neighboring pixels.	$\frac{\sum_i \sum_j (ij)p(i,j)-\mu_x\mu_y}{\sigma_x\sigma_y}$
Dissimilarity	Similar to contrast and inversely related to homogeneity.	$\sum_{n=0}^{N-1} n \left\{ \sum_{i=1}^{N} \sum_{j=1}^{N} p(i,j) \right\}$
Entropy	Shannon-diversity. High when the pixel values of the GLCM have varying values. Opposite of angular second moment.	$-\sum_i \sum_j p(i,j) \log(p(i,j))$
Homogeneity	A measure of homogenous pixel values across an image.	$\sum_i \sum_j \frac{1}{1+(i-j)^2} p(i,j)$
Mean	Gray level average in the GLCM window.	$\sum_{i,j=0}^{N-1} p(i,j)$
Variance	Gray level variance in the GLCM window.	$\sum_{i,j=0}^{N-1} p_{i,j}(i-\mu_i)^2$

[a] From Haralick et al. (1973).

2.5. Statistical analysis

To identify the set of most promising spectral bands and texture measures, we investigated the correlation structure among the different first- and second-order texture measures. We used Spearman rank correlation in this analysis because it is a non-parametric measure of statistical dependence that is robust to extreme values and monotonic relationships, which were evident from inspection of initial scatter plots (Zar, 1999). To investigate the degree of collinearity of texture measures with one another, we built Spearman rank matrices for the A) mean and B) standard deviation summary of three first and eight second-order texture measures derived from the air photo, and the C) mean and D) standard deviation of three first and eight second-order texture measures derived from Band 4 of the Landsat image. From this analysis, we learned the mean summaries of most texture measures were highly correlated ($|\rho|>0.7$, Appendices 1 and 2), but standard deviation summaries of texture measures showed a greater range of variation in their relationships with each other (Appendices 1 and 2).

In general, we eliminated from further analysis texture measures that were strongly correlated with other texture measures. We retained the sample-point mean and standard deviation from air photo data, Band 4, and the NDVI data. The sample-point mean values were identical to first-order mean, were mathematically less complex than second-order mean, and were not strongly correlated to other texture measures (Appendices 1 and 2). In practice, the values for both are often very similar since pixel values for neighboring cells tend to be similar. The difference is that sample-point mean or standard deviation values represent the mean or standard deviation of all pixels within a 100-m radius buffer around the sample point center, where the first-order mean is an average for a moving window (e.g., 3×3 window).

We also retained first-order entropy and first-order variance. The mean summaries of first-order entropy and variance were collinear and also strongly correlated to other texture measures. However, we selected these two texture measures because the standard deviation summaries were generally less correlated suggesting they uniquely capture textural heterogeneity (Appendices 1 and 2) and we hypothesized this may be related to variation in vegetation structure. Furthermore, entropy is a measure of pixel diversity calculated by the Shannon index (Table 1) which is a diversity index commonly used by ecologists. This may make entropy a texture measure that is more easily interpreted than, for example, angular second moment. We assumed that variance was an ecologically relevant texture measure since many ground-based vegetation quantification methods are designed to quantify habitat variation (e.g., vegetation structure). Additionally, we retained second-order contrast in order to determine if using a texture measure that is calculated using the GLCM, which quantifies 'neighborhood relationships' is superior to first-order measures in characterizing foliage-height diversity and horizontal vegetation structure.

To explore patterns of spatial autocorrelation of the dependent variables, we constructed semivariograms for both foliage-height diversity and horizontal vegetation structure among all sample points and within the three focal habitats (Legendre and Fortin, 1989). There were no apparent patterns of spatial autocorrelation for foliage-height diversity among and within habitats. There was slight spatial autocorrelation for horizontal vegetation structure within grassland habitats. However, there were no obvious patterns of spatial autocorrelation for horizontal vegetation structure within savanna and woodland sample points, and among all sample points.

To determine the amount of variance in foliage-height diversity that could be explained by image texture measures we used linear regression models. Normality of data distribution was checked using a Shapiro–Wilk test and QQ norm plots, and heteroscedasticity was checked using a Levene's test and visual inspection of residual plots (Zar, 1999). We applied logarithmic transformations for independent variables that were not normally distributed or that exhibited unequal variance. If the relationships appeared non-linear, we fit second-order polynomial models.

Horizontal vegetation structure data consistently failed to meet requirements of normality and equal variance, which are necessary assumptions for conducting linear regression, even when we applied logarithmic transformations. Therefore, to determine whether a relationship existed between image texture measures and horizontal vegetation structure, we used Spearman's rank correlation. All statistical analyses were completed using the R software package (R Development Core Team, 2005).

3. Results

As would be expected, grassland exhibited the lowest foliage-height diversity and horizontal vegetation structure and savanna and woodland both exhibited considerably greater mean and variation in foliage-height diversity and horizontal structure (Fig. 3A and B). The sample-point standard deviation and the mean summary of second-order contrast calculated from the air photo, as well as the sample-point mean from Band 4 and NDVI exhibited a similar pattern as the vegetation structure measures (Fig. 3C–F).

3.1. Relationships between air photo image texture measures and vegetation structure

Within grassland habitat, image texture was weakly correlated with foliage-height diversity (second-order contrast accounted for 11% of the variance, Table 2). However the standard deviation of first-order variance and second-order contrast were both moderately to strongly correlated with grassland horizontal vegetation structure ($\rho=0.71$ and $\rho=0.67$ respectively, Table 3). Within savanna habitat, foliage-height diversity was most strongly correlated with the mean summaries of both first-order variance and second-order contrast, which each accounted for approximately 30% of the variance (Table 2). Savanna horizontal vegetation structure was moderately correlated with the mean summary of both first-order entropy and second-order contrast ($\rho=0.41$, Table 3). Within woodland habitat, about 30% of variation in foliage-height diversity was accounted for

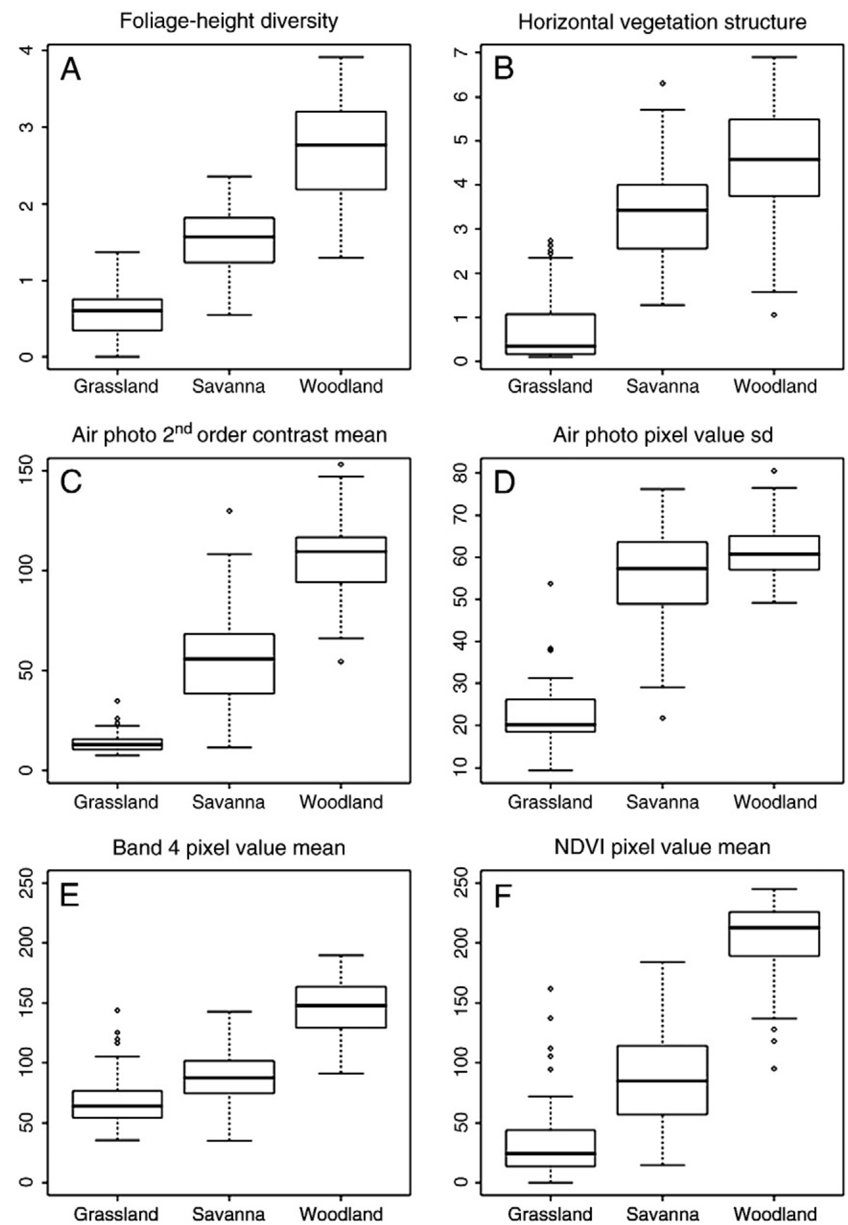

Fig. 3. Box plot summaries of vegetation structure and image texture characteristics in grassland, savanna, and woodland vegetation types. A) foliage-height diversity, B) horizontal vegetation structure (horizontal structure), C) 2nd order contrast calculated in a 3 × 3 pixel moving window on an infrared air photo, then summarized by the mean of pixels found within a 100 m radius circle, D) Infrared air photo pixel-values summarized by the standard deviation within a 100 m radius circle, E) Band 4 pixel-values summarized by the mean within a 100 m radius circle, and F) NDVI pixel-values summarized by the mean within a 100 m radius circle.

by the mean summary of second-order contrast (Table 2). Within woodland habitat, horizontal vegetation structure was not associated with any image texture measure.

Among habitats, about 80% of the variation in foliage-height diversity was associated with the mean of second-order contrast (Table 2). Horizontal vegetation structure was also strongly associated with second-order contrast, as well as the mean of first-order variance ($\rho = 0.73$ for both measures, Table 3). The relationship between foliage-height diversity and second order contrast was positive and linear, and the relationship was positive and curvilinear for first-order variance and horizontal vegetation structure (Fig. 4).

3.2. Relationships between Landsat image texture and vegetation structure

Within grassland habitat, 26% of the variation of foliage-height diversity was associated with the sample-point standard deviation of NDVI and second-order contrast of NDVI (Table 2), and horizontal vegetation structure was moderately correlated with the sample-point mean of NDVI ($\rho = 0.48$, Table 3). Within savanna, the association was weaker, with the sample-point mean of NDVI accounting for 10% of the variance in foliage-height diversity and the strongest association capturing only 16% of the variation (Band 4, Table 2). Horizontal vegetation structure was moderately correlated with the sample-point mean of NDVI ($\rho = 0.37$, Table 3). Within woodland habitat, however, about 60% of the variation in foliage-height diversity was associated with the sample-point mean summaries of both Band 4 and NDVI (Table 2). We did not find any significant correlations between any image texture measure and horizontal vegetation structure within woodlands (Table 3).

Among habitats, 71% and 74% of the variance in foliage-height diversity were associated with the sample-point mean of both NDVI and Band 4 (Table 2). The sample-point mean of NDVI was also strongly correlated with horizontal vegetation structure ($\rho = 0.70$,

Table 2
Univariate linear regression models of the strength of the relationship between foliage-height diversity and the mean (MEAN) and standard deviation (SD) of sample-point pixel values and 1st and 2nd order texture measures calculated from an infrared air photo, the near-infrared spectral band from a Landsat TM scene (Band 4), and a vegetation index, NDVI from a Landsat TM scene within three habitats (grassland, savanna, and woodlands) and among all three habitats (Global). Columns that are not populated with model metrics indicate that the assumptions of linear models could not be met.

	Grassland ($n=49$)		Savanna ($n=84$)		Woodland ($n=60$)		Global ($n=193$)	
	R^2	*p*-value	R^2	*p*-value	R^2	*p*-value	R^2	*p*-value
Air photo sample-point MEAN	−0.04	0.95	0.11	<0.01	0.04	0.12		
Air photo sample-point SD	0.00	0.35	0.28	<0.01				
Air photo first-order entropy MEAN	0.02	0.26	0.23[a]	<0.01	0.16[a]	<0.01	0.74[a]	<0.01
Air photo first-order entropy SD	0.00	0.36	0.20[a]	<0.01	0.14[a]	<0.01	0.73[a]	<0.01
Air photo first-order variance MEAN	0.05	0.12	0.32[a]	<0.01	0.18[a]	<0.01	0.74[a]	<0.01
Air photo first-order variance SD	0.09[a]	0.04	0.26[a]	<0.01	0.03	0.18		
Air photo second-order contrast MEAN	0.05[a]	0.11	0.31	<0.01	0.31	<0.01	0.79	<0.01
Air photo second-order contrast SD	0.11[a]	0.02	0.24	<0.01	0.06	0.04		
Band 4 sample-point MEAN	0.14	<0.01	0.16	<0.01	0.59	<0.01	0.74	<0.01
Band 4 sample-point SD	0.18	<0.01	0.00	0.32	0.04	0.11		
Band 4 first-order entropy MEAN	0.14[a]	0.01	0.06[a]	0.03	0.02	0.20	0.15[a]	<0.01
Band 4 first-order entropy SD	0.05	0.12	0.02	0.16	−0.03	0.90	0.12[a]	<0.01
Band 4 first-order variance MEAN	0.19[a]	<0.01	0.02	0.15	0.01	0.25	0.01	0.16
Band 4 first-order variance SD	0.15[a]	<0.01	0.00	0.32	0.00	0.48	0.01	0.13
Band 4 second-order contrast MEAN	0.09	0.03	0.01	0.17	0.03	0.09	0.00	0.31
Band 4 second-order contrast SD	0.02	0.17	0.06	0.02	0.00	0.40	0.00	0.41
NDVI sample-point MEAN	0.21	<0.01	0.10	<0.01	0.60	<0.01	0.71[a]	<0.01
NDVI sample-point SD	0.26	<0.01	−0.01	0.69	0.22	<0.01		
NDVI first-order entropy MEAN	−0.01	0.45	0.00	0.32	0.06	0.07		
NDVI first-order entropy SD	−0.02	0.82	0.00	0.38	0.04	0.11	0.04	0.01
NDVI first-order variance MEAN	−0.03	0.72	0.00	0.27	0.15	<0.01	0.00	0.84
NDVI first-order variance SD	−0.02	0.82	0.02	0.15	0.11	0.01	0.00	0.48
NDVI second-order contrast MEAN	0.26	<0.01	0.00	0.59	0.10	<0.01		
NDVI second-order contrast SD	0.12	<0.01	0.00	0.68	0.00	0.40		

[a] Model fit using the 2nd order polynomial.

Table 3). In contrast to the air photo findings, first- and second-order image texture measures calculated from Landsat data did not strongly characterize foliage-height diversity and horizontal vegetation structure among habitats, capturing only 15% of the variance in foliage-height diversity (Table 2), and they were weakly correlated with horizontal vegetation structure (Band 4 measures, $\rho=0.27$, Table 3). As was the case for air photo-based regression, the relationships between the sample-point mean of the Landsat data were positive and linear for foliage-height diversity, and positive and slightly curvilinear for horizontal vegetation structure among habitats (Fig. 4).

Table 3
Spearman rank correlations for horizontal vegetation structure against the mean (MEAN) and standard deviation (SD) of sample-point pixel values, and 1st and 2nd order texture measures calculated from an infrared air photo, the near-infrared spectral band from a Landsat TM scene (Band 4), and a vegetation index, NDVI from a Landsat TM scene within two habitats (grassland and savanna) and among all three habitats (Global). Woodland sample points were excluded from this table because no significant correlations could be found.

	Grassland ($n=49$)		Savanna ($n=84$)		Global ($n=193$)	
	ρ	*p*-value	ρ	*p*-value	ρ	*p*-value
Air photo sample-point MEAN	−0.24	0.09	−0.15	0.16	−0.45	<0.01
Air photo sample-point SD	0.37	0.01	0.40	<0.01	0.72	<0.01
Air photo first-order entropy MEAN	0.05	0.74	0.41	<0.01	0.71	<0.01
Air photo first-order entropy SD	−0.04	0.80	−0.39	<0.01	−0.70	<0.01
Air photo first-order variance MEAN	0.40	<0.01	0.39	<0.01	0.73	<0.01
Air photo first-order variance SD	0.71	<0.01	0.28	0.01	0.65	<0.01
Air photo second-order contrast MEAN	0.37	<0.01	0.41	<0.01	0.73	<0.01
Air photo second-order contrast SD	0.67	<0.01	0.33	<0.01	0.71	<0.01
Band 4 sample-point MEAN	0.08	0.56	0.32	<0.01	0.61	<0.01
Band 4 sample-point SD	0.40	<0.01	0.09	0.41	0.24	<0.01
Band 4 first-order entropy MEAN	0.33	0.02	0.13	0.25	0.27	<0.01
Band 4 first-order entropy SD	−0.15	0.32	−0.12	0.26	−0.21	<0.01
Band 4 first-order variance MEAN	0.45	<0.01	0.07	0.50	0.13	0.07
Band 4 first-order variance SD	0.45	<0.01	0.09	0.43	0.10	0.18
Band 4 second-order contrast MEAN	0.37	<0.01	0.00	0.95	0.06	0.38
Band 4 second-order contrast SD	0.31	0.03	−0.07	0.51	0.02	0.78
NDVI sample-point MEAN	0.48	<0.01	0.37	<0.01	0.70	<0.01
NDVI sample-point SD	0.37	<0.01	0.15	0.17	0.03	0.68
NDVI first-order entropy MEAN	−0.11	0.46	0.06	0.58	0.13	0.07
NDVI first-order entropy SD	0.09	0.53	−0.10	0.38	−0.13	0.08
NDVI first-order variance MEAN	0.17	0.25	−0.11	0.30	0.06	0.43
NDVI first-order variance SD	0.19	0.19	−0.10	0.36	0.05	0.47
NDVI second-order contrast MEAN	0.36	0.01	0.05	0.68	−0.13	0.07
NDVI second-order contrast SD	0.36	0.01	0.05	0.68	−0.14	0.06

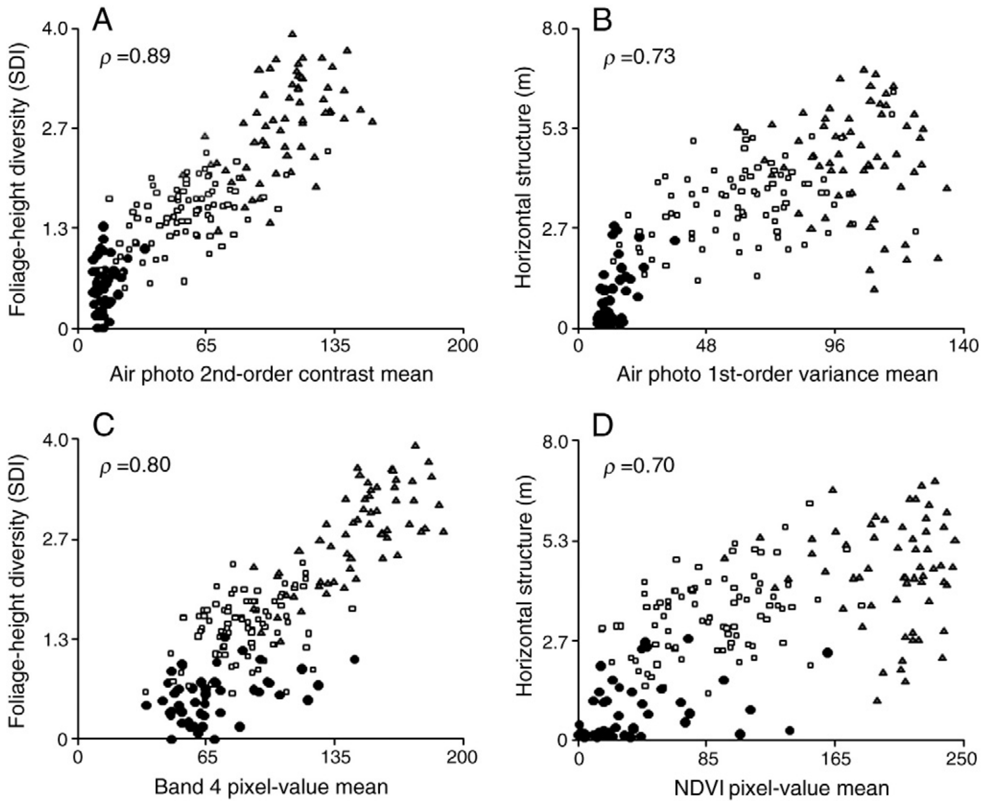

Fig. 4. Scatter plots depict best Spearman's rho correlation (ρ) of sample-point pixel value summaries, or image texture measures in predicting among-habitat (A) foliage-height diversity (Shannon diversity index), or (B) horizontal vegetation structure (meters). Sample-point pixel value summaries and image texture measures were calculated from an infrared air photo (row 1) and Band 4 and NDVI from a Landsat scene (row 2). The habitat of each plot is denoted as follows: grassland — solid black circle, savanna — hollow square, woodland — gray triangle.

4. Discussion

Vegetation structure greatly influences habitat selection by animals. However, ecologists lack adequate methods for measuring fine-scale heterogeneity of vegetation structure across broad extents. Our results suggest that within habitats, the relationships between image texture measures and foliage-height diversity and horizontal vegetation structure were low to moderately strong. Among habitats that differ in vegetation structure, such as the grassland–savanna–woodland mosaic that we studied, image texture of remotely sensed data characterizes foliage-height diversity and horizontal vegetation structure well. Image texture thus can capture gradients in vegetation structure that may be obscured by land cover classifications that assume that there are distinct vegetation categories.

Data derived from remotely sensed sources are useful for characterizing among habitat differences at broad extents (Turner et al., 2001). For example, Landsat data is commonly used to derive land-cover classifications which are useful for distinguishing the type and size of wildlife habitat (Kerr & Ostrovsky, 2003). However, determining within-habitat measures of vegetation structure heterogeneity is not possible with land-cover classifications, which is a shortcoming because within-habitat characteristics such as foliage-height diversity and horizontal vegetation structure are key elements determining habitat selection of animals (Morrison et al., 2006). LiDAR data appear adequate for discriminating differences in vegetation structure within habitats such as in pine forest (Clawges et al., 2008) and mixed-woodland (Lesak et al., 2011). Radar data have been applied to distinguish biomass metrics in a Northern Michigan forest (Bergen et al., 2009), and image texture has been used to characterize structural complexity within African montane forests (Estes et al., 2010). However, it has not been clear if image texture measures are useful for mapping within-habitat foliage-height diversity and horizontal vegetation structure. Our results suggest that image texture can capture up to a third of within-habitat foliage-height diversity and horizontal vegetation structure, and this is the most likely explanation for why image texture can successfully predict animal occurrences and abundances (Bellis et al., 2008; Estes et al., 2008, 2010; Hepinstall & Sader, 1997; St-Louis et al., 2006, 2009; Tuttle et al., 2006).

Furthermore, our results were consistent with previous studies that applied image texture to distinguish among-habitat vegetation structure patterns. While investigating brush encroachment in African savannas, Hudak and Wessman (2001) found high correlations among canopy cover and image texture, and between woody stem counts and image texture (1998). These African study sites were a mosaic of shrublands and savanna, similar in vegetation structure to our grassland–savanna–woodland study site. The mean summary of first-order standard deviation, calculated from high resolution air photos, was best related to the vegetation structural measurement, woody stem counts (Hudak & Wessman, 1998). First-order standard deviation is mathematically similar to first-order variance which we found to be related to foliage-height diversity within savanna habitats (Table 2), suggesting that this is a consistent measure of vegetation structure in ecosystems that include grass, shrub, and scattered tree (i.e., savanna) elements. In a managed boreal forest in Finland, second-order image texture measures, including contrast, calculated from high resolution air photos, were moderately correlated with vegetation structural metrics (Tuominen & Pekkarinen, 2005). The strength of the correlations among image-texture measures and vegetation structure metrics used in Finland corroborates our findings about the strength of the relationship between second order contrast and foliage-height diversity and horizontal vegetation structure and provides further evidence that image texture measures can discriminate among-habitat vegetation structural patterns, which can be useful for characterizing animal habitat across broad extents.

4.1. Relationships between image texture and vegetation structure

Our analysis highlighted differences among air photo- and satellite-derived data in the degree of association with foliage-height diversity and horizontal vegetation structure. The fine grained air photo better characterized foliage-height diversity and horizontal vegetation structure within savanna and among habitats than the satellite data. In contrast, the sample-point means from Band 4 and NDVI were better related to foliage-height diversity within grasslands and woodlands. This finding came as a surprise because in Finnish boreal forests, patterns of vegetation structure exhibited stronger relationships with image texture measures than with sample-point pixel-value summaries (Tuominen & Pekkarinen, 2005). Because of Tuominen and Pekkarinen's (2005) findings, we did not expect the sample point pixel-value mean and standard deviation summaries of Landsat-based NDVI to emerge as strong correlates of foliage-height diversity and horizontal vegetation structure because these metrics did not account for difference in scale (i.e., window size used to calculate image texture measures), which we hypothesized to be more strongly associated with variation in foliage-height diversity and horizontal vegetation structure. However, our results do coincide with evidence that NDVI characterizes vegetation metrics ranging from leaf-area index (Gamon et al., 1995) to plant species richness (Gould, 2000).

It is plausible that the air photo better explained foliage-height diversity and horizontal vegetation structure within savanna because the savanna habitats are characterized by abrupt changes in vegetation structural heterogeneity. Coarser grained Landsat data may not have been able to capture this variation. Moreover, among habitats, the air photo better captured the amount of variation in foliage-height diversity and horizontal vegetation structure. However, the sample point mean of Band 4 and the NDVI also characterized the among-habitat differences in the vegetation structure metrics well. Thus, the finer grained air photo appears to be a more useful image source than the Landsat data sources for characterizing habitat with abrupt changes in foliage-height diversity or horizontal vegetation structure such as savanna.

These results suggest that image texture measures calculated using a small window size from high resolution imagery and sample-point pixel values from Band 4 and NDVI were most strongly associated with foliage-height diversity and horizontal vegetation structure as it is measured on the ground. Other studies, in which there was a mis-match between the scale of ground data and the scale of texture processing, did not find correlations between image texture measures and vegetation metrics. For example, Lu and Batistella (2005) used vegetation data collected in sub-plots ranging from 1 m^2 to 100 m^2 to characterize tree-height, stem-height, and diameter at breast height of early successional and mature rainforest in Brazil across a highly fragmented landscape. These data were related to Landsat image texture calculated in window sizes capturing areas ranging from 150 m^2 to 750 m^2, but correlations were only moderate to poor. One explanation for why there were not stronger correlations in areas with high within-habitat heterogeneity may be that the scale of the ground-based measurements was not well matched to the scale of image texture calculation, resulting in moving windows that incorporated habitat data that was not sampled in the field plots.

4.2. Recommendations for use of texture measures

We suggest that if the goals of a study are to map and characterize foliage-height diversity and horizontal vegetation structure as a proxy for characterizing animal habitat in a heterogeneous landscape, investigators should match the scale of analysis (i.e., type and resolution of imagery and size of moving windows) with the spatial scale at which vegetation structure varies within habitats. If the goals of the study are to quantify vegetation structure at larger extents among heterogeneous habitats, in order to capture variation of adjacent habitats (i.e., landscape structural context), which may be influencing wildlife habitat selection, investigators should use larger window sizes. Furthermore, we suggest using the sample-point pixel value mean because this quantifies information of the 'local' area of interest (e.g., 100-m radius sample points), which related well with foliage-height diversity and horizontal vegetation structure among habitats.

Finally, due to the high correlation among remotely sensed variables, we recommend using a subset of first- and second-order texture measures. We suggest using one or two first-order texture measures such as variance, or entropy. We found these texture measures to capture approximately 30% of the variation of foliage-height diversity and horizontal vegetation structure within savannas. Additionally, these metrics were strongly related to the vegetation structure indices among habitats. Because these first-order texture measures are strongly correlated with second-order entropy and variance (Appendices 1 and 2), we recommend using the simpler first- and second-order image texture measures. We found second-order contrast to be highly related to foliage-height diversity among habitats, and others have characterized avian habitat using a closely related texture measure (i.e., second-order homogeneity, Tuttle et al., 2006). Thus, we recommend using a second-order texture measure such as contrast (Appendices 1 and 2), when characterizing foliage-height diversity or horizontal vegetation structure. Finally, since we found the sample-point pixel value mean of Band 4 and NDVI to be strongly related to foliage-height diversity among habitats and within woodlands, and since these measures are highly collinear with first- and second-order mean, we suggest using these measures when using Landsat data to characterize foliage-height diversity and horizontal vegetation structure patterns across broad extents.

5. Conclusions

Ecologists need effective tools for measuring habitat at both fine scales and broad extents. Field-based methods for fine scale habitat quantification are well established. However, efficient methods that characterize fine grained habitat features across broad extents are lacking. The results of our study suggest that sample-point pixel value summaries and image texture calculated from remotely sensed data characterize 26–60% of the variation of foliage-height diversity within grassland, savanna, and woodland habitats, and up to 79% among habitats. Within and among habitats, sample-point pixel values and image texture were correlated with 70% of horizontal vegetation structure. These findings are important because wildlife diversity, richness, and distributions are linked to foliage-height diversity and horizontal vegetation structure. We provide evidence that remotely sensed data can be used to characterize foliage-height diversity and horizontal vegetation structure and thus is a tool for mapping wildlife habitat across broad spatial extents.

Acknowledgments

We would like to thank our field assistants, C. Rockwell, A. Nolan, B. Summers, H. Llanas, S. Grover, P. Kearns, and A. Derose-Wilson, for their tireless help in collecting many foliage-height diversity measurements. T. Wilder and S. Vos provided valuable logistical support while in the field at Fort McCoy. D. Aslesen provided the remotely sensed data sources. C. Gratton, R. Jackson, and C. Ribic provided valuable feedback during manuscript preparation. Two anonymous reviewers provide very constructive and helpful comments on an earlier version of this manuscript. We are grateful for funding support of the Strategic Environmental Research and Development Program for this research.

Appendix 1

Spearman rank correlation coefficients of three 1st order and eight 2nd order texture measures calculated from an infrared air photo in a 3 × 3 moving window in a 100 m radius buffer around 193 sample points. Above the diagonal are texture measures summarized by the standard deviation. Below the diagonal are texture measures summarized by the mean.

Measure			1st order			2nd order							
	Texture	Infrared†	ENT	MN	VAR	CON	COR	DIS	ENT	HOM	MN	ASM	VAR
	Infrared†		−0.75	0.97	0.89	0.88	−0.75	0.85	−0.72	0.06	0.97	−0.73	0.89
1st order	ENT	−0.46		−0.62	−0.70	−0.81	0.95	−0.62	0.99	0.51	−0.62	1	−0.70
	MN	1	−0.46		0.84	0.78	−0.62	0.83	−0.58	0.13	1	−0.59	0.83
	VAR	−0.51	0.95	−0.5		0.95	−0.68	0.96	−0.66	0.05	0.84	−0.68	1
2nd order	CON	−0.51	0.96	−0.51	0.99		−0.80	0.93	−0.77	−0.13	0.78	−0.79	0.95
	COR	−0.64	0.95	−0.64	0.93	0.94		−0.63	0.93	0.45	−0.62	0.94	−0.68
	DIS	−0.51	0.97	−0.5	0.99	1	0.95		−0.57	0.21	0.83	−0.59	0.96
	ENT	−0.41	0.99	−0.41	0.93	0.93	0.93	0.95		0.54	−0.58	1	−0.66
	HOM	0.48	−0.99	0.47	−0.97	−0.98	−0.96	−0.99	−0.98		0.13	0.54	0.05
	MN	1	−0.46	1	−0.50	−0.51	−0.64	−0.5	−0.41	0.47		−0.60	0.83
	ASM	0.45	−1	0.45	−0.95	−0.96	−0.95	−0.97	−0.99	0.99	0.45		−0.68
	VAR	−0.51	0.95	−0.5	1	0.99	0.93	0.99	0.92	−0.97	−0.50	−0.95	

Infrared† = sample-point pixel values (no moving window analysis).

First-order measures: ENT = entropy, MN = mean, VAR = variance — second-order measures: CON = contrast, COR = correlation, DIS = dissimilarity, ENT = entropy, HOM = homogeneity, MN = mean, ASM = angular second moment, VAR = variance.

Appendix 2

Spearman rank correlation coefficients of three 1st order and eight 2nd order texture measures calculated from the near-infrared band (Band 4) of a Landsat scene in a 3 × 3 moving window in a 100 m radius buffer around 193 sample points. Above the diagonal are texture measures summarized by the standard deviation. Below the diagonal are texture measures summarized by the mean.

Measure			1st order			2nd order							
	Texture	Band 4†	ENT	MN	VAR	CON	COR	DIS	ENT	HOM	MN	ASM	VAR
	Band 4†		−0.35	0.92	0.77	0.67	0.59	0.58	−0.39	0.42	0.94	−0.52	0.80
1st order	ENT	0.50		−0.30	−0.25	−0.22	−0.34	−0.07	0.65	0.06	−0.28	0.65	−0.24
	MN	0.99	0.51		0.78	0.61	0.47	0.56	−0.29	0.43	0.96	−0.41	0.75
	VAR	0.29	0.77	0.31		0.75	0.51	0.68	−0.23	0.50	0.75	−0.36	0.95
2nd order	CON	0.30	0.68	0.29	0.80		0.48	0.93	−0.20	0.73	0.63	−0.33	0.80
	COR	−0.30	−0.64	−0.30	−0.63	−0.62		0.41	−0.27	0.31	0.50	−0.38	0.53
	DIS	0.36	0.74	0.35	0.74	0.94	−0.62		−0.02	0.89	0.57	−0.13	0.73
	ENT	0.46	0.85	0.46	0.73	0.76	−0.68	0.86		0.19	−0.31	0.95	−0.25
	HOM	−0.39	−0.76	−0.38	−0.68	−0.88	0.62	−0.98	−0.88		0.43	0.07	0.55
	MN	1	0.50	0.99	0.30	0.31	−0.30	0.37	0.47	−0.40		−0.44	0.78
	ASM	−0.46	−0.84	−0.46	−0.70	−0.74	0.66	−0.85	−0.99	0.88	−0.46		−0.39
	VAR	0.33	0.75	0.33	0.95	0.84	−0.67	0.79	0.78	−0.74	0.34	−0.76	

Band 4† = sample-point pixel values of Band 4.

First-order measures: ENT = entropy, MN = mean, VAR = variance — second-order measures: CON = contrast, COR = correlation, DIS = dissimilarity, ENT = entropy, HOM = homogeneity, MN = mean, ASM = angular second moment, VAR = variance.

References

Anderson, J. R. (1976). *A land use and land cover classification system for use with remote sensor data.* U.S Geological Survey Professional Paper 964. Reston, VA, USA: U.S. Geological Survey.

August, P. V. (1983). The role of habitat complexity and heterogeneity in structuring tropical mammal communities. *Ecology*, *64*, 1495–1507.

Bailey, S. A., Horner-Devine, M. C., Luck, G., Moore, L. A., Carney, K. M., Anderson, S., et al. (2004). Primary productivity and species richness: relationships among functional guilds, residency groups and vagility classes at multiple spatial scales. *Ecography*, *27*, 207–217.

Bellis, L. M., Pidgeon, A. M., Radeloff, V. C., St-Louis, V., Navarro, J. L., & Martella, M. B. (2008). Modeling habitat suitability for Greater Rheas based on satellite image texture. *Ecological Applications*, *18*, 1956–1966.

Bergen, K. M., Goetz, S. J., Dubayah, R. O., Henebry, G. M., Hunsaker, C. T., Imhoff, M. L., et al. (2009). Remote sensing of vegetation 3D structure for biodiversity and habitat: Review and implications for lidar and radar spaceborne missions. *Journal of Geophysical Research*, *114*, G00E06. doi:10.1029/2008JG000883.

Bestelmeyer, B. T., & Wiens, J. A. (2001). Ant biodiversity in semiarid landscape mosaics: The consequences of grazing vs. natural heterogeneity. *Ecological Applications*, *11*, 1123–1140.

Beyer, H. L. (2004). *Hawth's analysis tools for ArcGIS.*

Clawges, R., Vierling, K. I., Vierling, L., & Rowell, E. (2008). The use of airborne lidar to assess avian species diversity, density, and occurrence in a pine/aspen forest. *Remote Sensing of Environment*, *112*, 2064–2073.

Coburn, C. A., & Roberts, A. C. B. (2004). A multiscale texture analysis procedure for improved forest stand classification. *International Journal of Remote Sensing*, *25*, 4287–4308.

Cody, M. L. (1981). Habitat selection in birds: The roles of vegetation structure, competitors, and productivity. *Bioscience*, *31*, 107–113.

Cody, M. L. (1985). *Habitat selection in birds* (pp. 558). San Diego, CA, USA: Academic Press.

Culbert, P. D., Pidgeon, A. M., St-Louis, V., Bash, D., & Radeloff, V. C. (2009). The impact of phenological variation on texture measures of remotely sensed imagery. *IEEE Journal of Selected Topics in Applied Earth Observations and Remote Sensing*, *2*, 299–309.

Dobrowski, S. Z., Safford, H. D., Ben Cheng, Y., & Ustin, S. L. (2008). Mapping mountain vegetation using species distribution modeling, image-based texture analysis, and object-based classification. *Applied Vegetation Science*, *11*, 499–508.

ESRI, Redlands, California, USA (Ed.), (2006). ArcGIS 9.1. Redlands, CA, USA.

Estades, C. F. (1997). Bird-habitat relationships in a vegetational gradient in the Andes of central Chile. *The Condor*, *99*, 719–727.

Estes, L. D., Okin, G. S., Mwangi, A. G., & Shugart, H. H. (2008). Habitat selection by a rare forest antelope: A multi-scale approach combining field data and imagery from three sensors. *Remote Sensing of Environment*, *112*, 2033–2050.

Estes, L. D., Reillo, P. R., Mwangi, A. G., Okin, G. S., & Shugart, H. H. (2010). Remote sensing of structural complexity indices for habitat and species distribution modeling. *Remote Sensing of Environment*, *114*, 792–804.

Gamon, J. A., Field, C. B., Goulden, M. L., Griffin, K. L., Hartley, A. E., Joel, G., et al. (1995). Relationships between NDVI, canopy structure, and photosynthesis in three Californian vegetation types. *Ecological Applications*, *5*, 28–41.

Gausman, H. W. (1977). Reflectance of leaf components. *Remote Sensing of Environment*, *6*, 1–9.

Ge, S., Carruthers, R., Gong, P., & Herrera, A. (2006). Texture analysis for mapping *Tamarix parviflora* using aerial photographs along the Cache Creek, California. *Environmental Monitoring and Assessment*, *114*, 65–83.

Gillespie, T. W., Foody, G. M., Rocchini, D., Giorgi, A. P., & Saatchi, S. (2008). Measuring and modelling biodiversity from space. *Progress in Physical Geography*, *32*, 203–221.

Goetz, S. J., Steinberg, D., Betts, M. G., Holmes, R. T., Doran, P. J., Dubayah, R., et al. (2010). Lidar remote sensing variables predict breeding habitat of a neotropical migrant bird. *Ecology*, *91*, 1569–1576.

Goetz, S., Steinberg, D., Dubayah, R., & Blair, B. (2007). Laser remote sensing of canopy habitat heterogeneity as a predictor of bird species richness in an eastern temperate forest, USA. *Remote Sensing of Environment*, *108*, 254–263.

Gould, W. (2000). Remote sensing of vegetation, plant species richness, and regional biodiversity hotspots. *Ecological Applications*, *10*, 1861–1870.

Greenstone, M. H. (1984). Determinants of web spider species diversity: Vegetation structural diversity vs. prey availability. *Oecologia*, *62*, 299–304.

Hall-Beyer, M. (2007). *The GLCM tutorial home page. Current Version 2.10.*

Haralick, R. M. (1979). Statistical and structural approaches to texture. *Proceedings of the IEEE*, *67*, 786–804.

Haralick, R. M., Shanmugam, K., & Dinstein, I. H. (1973). Textural features for image classification. *Systems, Man and Cybernetics, IEEE Transactions on*, *3*, 610–621.

Hepinstall, J. A., & Sader, S. A. (1997). Using Bayesian statistics, thematic mapper satellite imagery, and breeding bird survey data to model bird species probability of occurrence in Maine. *Photogrammetric Engineering and Remote Sensing*, *63*, 1231–1237.

Hinsley, S. A., Hill, R. A., Bellamy, P. E., & Balzter, H. (2006). The application of LiDAR in woodland bird ecology: climate, canopy structure, and habitat quality. *Photogrammetric Engineering and Remote Sensing*, *72*, 1399.

Hudak, A. T., & Wessman, C. A. (1998). Textural analysis of historical aerial photography to characterize woody plant encroachment in South African savanna. *Remote Sensing of Environment*, *66*, 317–330.

Hudak, A. T., & Wessman, C. A. (2001). Textural analysis of high resolution imagery to quantify bush encroachment in Madikwe Game Reserve, South Africa, 1955–1996. *International Journal of Remote Sensing*, *22*, 2731–2740.

Hutto, R. L. (1985). Habitat selection by nonbreeding, migratory land birds. In M. L. Cody (Ed.), *Habitat selection in birds* (pp. 455–476). Orlando, Florida, USA: Academic Press, Inc.

Karr, J. R., & Roth, R. R. (1971). Vegetation structure and avian diversity in several new world areas. *The American Naturalist*, *105*, 423.

Kerr, J. T., & Ostrovsky, M. (2003). From space to species: Ecological applications for remote sensing. *Trends in Ecology & Evolution*, *18*, 299–305.

Kuplich, T. M., Curran, P. J., & Atkinson, P. M. (2005). Relating SAR image texture to the biomass of regenerating tropical forests. *International Journal of Remote Sensing*, *26*, 4829–4854.

Laurent, E. J., Shi, H., Gatziolis, D., LeBouton, J. P., Walters, M. B., & Liu, J. (2005). Using the spatial and spectral precision of satellite imagery to predict wildlife occurrence patterns. *Remote Sensing of Environment*, *97*, 249–262.

Lee, P. F., Ding, T. S., Hsu, F. H., & Geng, S. (2004). Breeding bird species richness in Taiwan: Distribution on gradients of elevation, primary productivity and urbanization. *Journal of Biogeography*, *31*, 307–314.

Legendre, P., & Fortin, M. -J. (1989). Spatial pattern and ecological analysis. *Vegetatio*, *80*, 107–138.

Lesak, A. A., Radeloff, V. C., Hawbaker, T. J., Pidgeon, A. M., Gobakken, T., & Contrucci, K. (2011). Modeling forest songbird species richness using LiDAR-derived measures of forest structure. *Remote Sensing of Environment*, *115*, 2823–2835.

Lu, D., & Batistella, M. (2005). Exploring TM image texture and its relationships with biomass estimation in Rondônia, Brazilian Amazon. *Acta Amazonica*, *35*, 249–257.

MacArthur, R. H., & MacArthur, J. W. (1961). On bird species diversity. *Ecology*, *42*, 595–599.

Martin, T. E. (1993). Nest predation and nest sites. *Bioscience*, *43*, 523–532.

Martin, T. E., Paine, C. R., Conway, C. J., Hochachka, W. M., & Jenkins, W. (1997). *BBIRD Field Protocol. Montana Cooperative Wildlife Research Unit.* Missoula: University of Montana Available Online. http://pica.Wru.Umt.edu/BBIRD/protocol/Protocol.htm accessed April 5, 2007.

McShea, W. J. (2000). The influence of acorn crops on annual variation in rodent and bird populations. *Ecology*, *81*, 228–238.

Morrison, M. L., Marcot, B. G., & Mannan, R. W. (2006). *Wildlife-habitat relationships: Concepts and applications.* Washington, DC, USA: Island Press.

Murdoch, W. W., Evans, F. C., & Peterson, C. H. (1972). Diversity and pattern in plants and insects. *Ecology*, *53*, 819–829.

Naugle, D. E., Higgins, K. F., Nusser, S. M., & Johnson, W. C. (1999). Scale-dependent habitat use in three species of prairie wetland birds. *Landscape Ecology*, *14*, 267–276.

Nudds, T. D. (1977). Quantifying the vegetative structure of wildlife cover. *Wildlife Society Bulletin*, *5*, 113–117.

Patterson, M. P., & Best, L. B. (1996). Bird abundance and nesting success in Iowa CRP fields: The importance of vegetation structure and composition. *The American Midland Naturalist*, *135*, 153–167.

Pidgeon, A. M., Mathews, N. E., Benoit, R., & Nordheim, E. V. (2001). Response of avian communities to historic habitat change in the northern Chihuahuan desert. *Conservation Biology*, *15*, 1772–1789.

R Development Core Team (2005). *A language and environment for statistical computing.* Vienna, Austria: R Foundation for Statistical Computing3-900051-07-0.

Robinson, S. K., & Holmes, R. T. (1984). Effects of plant species and foliage structure on the foraging behavior of forest birds. *The Auk*, *101*, 672–684.

Rotenberry, J. T., & Wiens, J. A. (1980). Habitat structure, patchiness, and avian communities in North American steppe vegetation: A multivariate analysis. *Ecology*, *61*, 1228–1250.

Roughgarden, J., Running, S. W., & Matson, P. A. (1991). What does remote sensing do for ecology? *Ecology*, *72*, 1918–1922.

Seavy, N. E., Viers, J. H., & Wood, J. K. (2009). Riparian bird response to vegetation structure: A multiscale analysis using LiDAR measurements of canopy height. *Ecological Applications*, *19*, 1848–1857.

Seto, K. C., Fleishman, E., Fay, J. P., & Betrus, C. J. (2004). Linking spatial patterns of bird and butterfly species richness with Landsat TM derived NDVI. *International Journal of Remote Sensing*, *25*, 4309–4324.

Southwood, T. R. E., Brown, V. K., & Reader, P. M. (1979). The relationships of plant and insect diversities in succession. *Biological Journal of the Linnean Society*, *12*, 327–348.

St-Louis, V., Pidgeon, A. M., Clayton, M. K., Locke, B. A., Bash, D., & Radeloff, V. C. (2009). Satellite image texture and a vegetation index predict avian biodiversity in the Chihuahuan desert of New Mexico. *Ecography*, *32*, 468–480.

St-Louis, V., Pidgeon, A. M., Radeloff, V. C., Hawbaker, T. J., & Clayton, M. K. (2006). High-resolution image texture as a predictor of bird species richness. *Remote Sensing of Environment*, *105*, 299–312.

Szép, T., Mřller, A. P., Piper, S., Nuttall, R., Szabó, Z. D., & Pap, P. L. (2006). Searching for potential wintering and migration areas of a Danish barn swallow population in South Africa by correlating NDVI with survival estimates. *Journal of Ornithology*, *147*, 245–253.

Tews, J., Brose, U., Grimm, V., Tielbörger, K., Wichmann, M. C., Schwager, M., et al. (2004). Animal species diversity driven by habitat heterogeneity/diversity: The importance of keystone structures. *Journal of Biogeography*, *31*, 79–92.

Thuiller, W., Araujo, M. B., & Lavorel, S. (2004). Do we need land-cover data to model species distributions in Europe? *Journal of Biogeography*, *31*, 353–361.

Tucker, C. J. (1979). Red and photographic infrared linear combinations for monitoring vegetation. *Remote Sensing of Environment*, *8*, 127–150.

Tuominen, S., & Pekkarinen, A. (2005). Performance of different spectral and textural aerial photograph features in multi-source forest inventory. *Remote Sensing of Environment*, *94*, 256–268.

Turner, M. G., Gardner, R. H., & O'Neill, R. V. (2001). *Landscape ecology in theory and practice: Pattern and process* (pp. 401). New York, NY, USA: Springer.

Turner, W., Spector, S., Gardiner, N., Fladeland, M., Sterling, E., & Steininger, M. (2003). Remote sensing for biodiversity science and conservation. *Trends in Ecology & Evolution*, *18*, 306–314.

Tuttle, E. M., Jensen, R. R., Formica, V. A., & Gonser, R. A. (2006). Using remote sensing image texture to study habitat use patterns: A case study using the polymorphic white-throated sparrow (*Zonotrichia albicollis*). *Global Ecology and Biogeography*, *15*, 349–357.

Venier, L. A., Pearce, J., McKee, J. E., McKenney, D. W., & Niemi, G. J. (2004). Climate and satellite-derived land cover for predicting breeding bird distribution in the Great Lakes Basin. *Journal of Biogeography*, *31*, 315–331.

Vierling, K. T., Vierling, L. A., Gould, W. A., Martinuzzi, S., & Clawges, R. M. (2008). Lidar: shedding new light on habitat characterization and modeling. *Frontiers in Ecology and the Environment*, *6*, 90–98.

Wiens, J. A., & Rotenberry, J. T. (1981). Habitat associations and community structure of birds in shrubsteppe environments. *Ecological Monographs*, *51*, 21–42.

Zar, J. H. (1999). *Biostatistical analysis* (pp. 663). Upper Saddle River, NJ, USA: Prentice-Hall.

Zhang, C., & Franklin, S. E. (2002). Forest structure classification using airborne multispectral image texture and kriging analysis. *IEEE*, *4*, 2522–2524.